

Evaluation of Reduced Graphene Oxide-Zeolitic Imidazolate Framework onto Nanofibers

Nurul Faizatul Nadia binti Khalid and Noor Fitrah binti Abu Bakar

Faculty of Chemical Engineering, Universiti Teknologi MARA

Abstract— Nowadays, with the increasing of the industry in world, many heavy metal related issues is arise and increase every year. Researcher have been trying to incorporate the sensor with nanomaterial to increase the detection properties of the sensor and making those sensor to be more selective and sensitive. The material that is usually incorporated with heavy metal sensor is graphene oxide (GO) because of the thermal properties but it have some issue such as limitation when using in many electronic devices. Thus, for this study, reduced graphene oxide (rGO) is used rather than GO because the good electric properties and lower cost to fabricated, but the rGO have issue with the sensing response and the times for the recovery. Hence, rGO is combined with zeolitic imidazolate framework (ZIF) to improve the sensing properties of rGO. Therefore, the combination of rGO-ZIF is incorporated with PEI to increase the conductivity of the electrospun fiber mats produced. The fiber mats is then analyzed by using porosity test, contact angle test, and conductivity test. Results from this analysis shows that the conductivity of the electrospun PEI is increased with the addition of rGO-ZIF which is from 3.0764×10^{-6} S/cm without addition of rGO-ZIF to 2.3600×10^{-4} S/cm with addition of rGO-ZIF at 0.3 wt % concentration of rGO-ZIF.

Keywords— *electrospinning, reduced graphene oxide, zeolitic imidazolate framework, polyetherimide, sensor*

I. INTRODUCTION

Heavy metal such as arsenic, mercury, cadmium, chromium, and lead are substances that can pollute the environment. This heavy metal is causing by the industrial effluent discharge of the activities such as electroplating, mining, fabrication of batteries and microelectronics [1]. The heavy metal can affect the health of human beings, causing heavy metal poisoning in the body. According to [2], heavy metal is a substances that can be enhanced many times and when this heavy metal is consumed by aquatic animals and plants, this will causing heavy metal pile up into them. Later, when this animals and plants is consumed by the human, heavy metal poisoning will occurred and causing disease like Minamata disease and worst scenario is death.

The sources of heavy metal are usually from the industry plant. However, in the country that do not have industrial plant, the sources of heavy metal are coming from landfills. In developing country, landfills is the key technique in handling household waste and the waste separation system is also absent thus the many hazardous material are transferred to the landfills. Heavy metal stays in the environment for a very long time because it is not decomposed by the microorganism and chemicals making it more dangerous for long term [3]. The study from [4], state that heavy metal can contaminate agricultural soil by initiation of dangerous

substances through water, air or the accumulation on or in soil above the allowable concentration. Contamination of soil by heavy metals will result in long term period that will affect the fertility and soil quality as well as causing toxicity to the plants and to the person and animal who consume it. Consequences of heavy metal can be carcinogenic and mutagenic. Children who expose to the heavy metals toxicity will having neurological damage such as learning difficulties. Moreover, exposure to the lead can result in epileptic attacks, mental retardation, and behavioral disorders.

Removal of heavy metal is carried out to reduce the effect of this substances to environment as well as human beings. Nowadays, the new technologies that involve the sensor is introduced to the heavy metal removal process. This technologies is used because it give several advantages such are high sensitivity, rapid detection, ease of use and suitability for in-situ, real time and continuous monitoring of the heavy metal elements. In general, sensor contain of sensing unit and transduction unit that use to convert the information detected into signal such are electrical and optical signal [5]. There are several type of sensor available such are optical sensor, electrochemical sensor, and field-effect transistor (FET) [6].

There are several characteristics that is crucial in sensor such are the sensitivity, selectivity, response time, reusability, long-term stability and cost that causing the selection of the sensor is thoroughly done based on the requirement of the elements that need to be detected. Recently, many sensor have been modified for the environment control and this sensors have been engaged with several micro-material and nanomaterial to get the characteristics of this materials. Example of the materials are nanocarbon materials and polymers [5].

Generally, modified heavy metal sensor that consists of nanomaterial will have the membrane and solvents. As for this research, the sensor is made up form reduced graphene oxide hybridized with zeolitic imidazolate framework (ZIF) that act as membrane to the polyetherimide (PEI) that act as solvent. Reduced graphene oxide (rGO) is synthesized from graphene which is component that have two-dimensional carbon nanomaterial which contain a single layer of sp^2 -bonded carbon atoms. Synthesizing of the graphene oxide (GO) is done because of some lacking in the component which are the lack of band gap and limitation of the GO in some of the electrical devices. Thus, rGO is produced because of electrical properties that give more conductivity on some electrical devices. Besides, it can be produced on the large scale at lower cost compared to the GO [7].

ZIF is a metal organic framework that consist of imidazolate linker and metal ions which have porous attribute and many range of capability such as thermal and chemical stabilities. Thus it causing ZIF to have broad range of applications such as separation, catalysis and sensing. Besides, ZIF is also breed of MOF that consist of M-Im-M where the M indicates Zn and Co while Im indicate imidazolate linker where it making ZIF have zeolite and MOF properties which make the ZIF have high crystallinities, ultrahigh surface areas, and many [8]. According to [9], ZIF have many advantages compared to other zeolites which ZIF is more flexible in surface adjustment. Besides. It also permits rational design of surface properties. Moreover, MOF is

developing as porous material that have high surface area, rich uncoordinated metal ions and tunable pore size that is popular for adsorption of heavy metals ions such as cadmium and radioactive metal ions [10].

Electrospinning is the popular technique in producing nanofiber polymer. Electrostatic force is employed to a polymer solution to produce fibers with diameter range from microns to nanometer [11]. The basic builds up of electrospinning consist three setup which are high voltage power supply, spinneret and a collector. According to [12], there are many characteristic of the electrospun fiber. First, it will produce varies diameter of nanofiber but it depends on solution concentration. The more concentration will produce bigger diameter. Next is the porosity of the nanofiber produce. Electrospinning technique will produce fiber with thinner diameter and causing the surface area to increase compared to usual technique. Besides, it also produce fiber with more smooth structure when high concentration solution is used. For this research, the polymer used as a substrate is polyetherimide (PEI) for the heavy metal sensor because of the properties of PEI which is a vague, thermoplastic polymer with high resistance to heat and high tensile strength [13]. The study of [14] state that PEI is the high-performance polymer which possesses a high T_g of 215°C but when introduce to the fillers, the viscosity of the polymers increasing which make the PEI not favorable. Moreover, this study also shows that PEI have low electrical conductivity which is 1.2×10^{-19} S/cm. Thus, when adding with another material such as graphene, the conductivity of the PEI increased to 3.9×10^{-10} S/cm.

II. METHODOLOGY

A. Materials

Polyetherimide (PEI) is purchased from Sigma-Aldrich with density of 1.27 g/mL. The solution of the polymer is prepared using N-Methyl-c-Pyrrolidone (NMP) and both are purchased from R&M Chemicals.

B. Preparation of Polyetherimide (PEI)

PEI is weighed about 1g, 2g, and 3g to make 10 wt %, 20 wt %, and 30 wt % of PEI respectively. Then the weighted PEI is dissolved with the NMP solution at 10 mL. The solution is stirred vigorously at 70°C for 4 hours or more depends on the concentration.

C. Preparation of Reduced Graphene Oxide-Zeolitic Imidazolate Framework/PEI Solution

The rGO-ZIF [15] is dissolved into the NMP solvents with the same volume as the PEI preparation using sonicator. Concentration of the rGO-ZIF used is varied with 0.1 wt %, 0.3 wt % and 0.5 wt %. After that, the solution of the rGO-ZIF are dissolved into the PEI solution using magnetic stirrer for about 1 hour.

D. Electrospinning Method

Firstly, 5 mL of disposable plastic syringe is cleaned using distilled water to remove all the impurities. Then, 2 mL of the 10 wt % PEI solution is injected into it. A needle with diameter of 0.5 mm is attached at the syringe and the electrospinning process is set up as the Fig 1. High voltage current is supplied at the set up and the distance of the tip to collector is set to be 20 cm. Besides, the flow rate of the solution is fixed to 0.8 mL/hr and the voltage used is -20 kV to get the uniform Taylor cone jet. At the collector, screen-printed carbon electrode (SPCE) is attached to collect the electrospun fibers for conductivity analysis. The SPCE is wrapped with aluminium foil and only working electrode is left unwrapped so that the fibers can attach onto it. Then, process is carried out for two and half hours under consistent temperature and humidity.

Lastly, the product of the electrospinning which is electrospun fibers is dried at room temperature and then placed in the desiccator. Steps is repeated for PEI with different concentration and rGO-ZIF-PEI with different concentration.

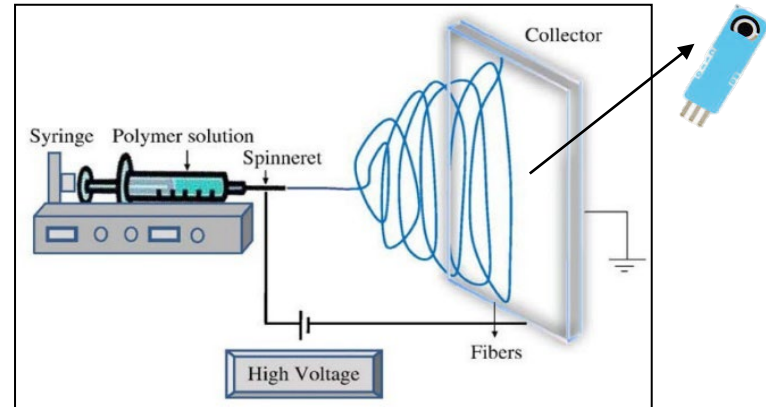


Fig. 1: Electrospinning Set-up

E. Porosity and Electrolyte Uptake Test

To measure the porosity of the electrospun fiber mats, n-butanol is used. The mats is cut into square shape with dimension 2 cm × 2 cm and then soaked into n-butanol for 2 hours at room temperature. After that, the mats is removed from the n-butanol solutions and dried with tissue before weighed. Porosity if the fiber mats can be calculated using formula (1).

$$\text{Porosity} = (m_b / \rho_b) / [(m_b / \rho_b) + (m_p / \rho_p)] \times 100\% \quad \dots(1)$$

Where m_b and m_p are the mass of n-butanol and electrospun fiber mats respectively and ρ_b and ρ_p are the density of the n-butanol and polymer which is PEI. To obtain m_p , the square shape that cuts from fiber mats before soaked into n-butanol is weighed while m_b is obtain form the cuts that is soaked with n-butanol. Besides, the water uptake also can be measured using the equation (2).

$$\text{Uptake} = (W_1 - W_0) / W_0 \times 100\% \quad \dots(2)$$

Where W_1 is the weight of the fiber mats soaked in n-butanol and W_0 is the weight of the fiber mats before soaked in n-butanol.

F. Electrochemical Impedance Spectroscopy (EIS)

The conductivity test of the electrospun fiber mat is done using Electrochemical Impedance Spectroscopy (EIS). Fiber mats are electrospun onto the screen-printed carbon electrode (SPCE). The SPCE is wrapped in aluminium foil first before the fibers is electrospun on it but the working electrode is allow unwrapped so that the electrospun fiber can attach onto it. EIS characterization is performed in acetate buffer solution with pH 4.6 and the frequency is varied between 100 MHz to 100 kHz. After that, the conductivity of the polymer is then determined using the formula (3).

$$\sigma = L / (R_b \times A) \quad \dots(3)$$

Where L is the thickness in cm, R_b is the bulk resistance in ohm (Ω), and A is the contact area between electrospun fiber mats with electrodes [16].

G. Water Contact Angle Test

This test is conducted using goniometer. Goniometer is used to capture the profile of a water on a solid surface by optical subsystem. The glass syringe is filled with distilled water and then the syringe is placed on the push block. After that, charge couple device (CCD) and illumination lamps are turned on. The electrospun samples which is cut uniformly are placed on the sample stage and the syringe knob is opened for the water to fall onto the sample. Lastly, by using the software, the contact angle is measured between the liquid droplet and fiber surface.

H. Field Emission Scanning Electron Microscopy (FESEM)

For morphology analysis, Zeiss Supra is used with gold coating. Three different magnification was used to obtain the clear image of the electrospun nanofibers which are 3 KX, 5 KX and 10 KX.

III. RESULTS AND DISCUSSION

A. Porosity Analysis

Porosity of electrospun fibers is the ratio of the pore volume of the electrospun fibers to the total volume of the electrospun fibers which is expressed in percentage [17]. According to [18], solvent play an important role when preparing the polymer solution because it will affect the spinnability. The solvent chosen must have properties such as good vapor pressure and boiling point. Thus, NMP is chose over DMF because the boiling point of NMP is higher than DMF. Lower boiling point will cause the solvent evaporate easily during electrospinning. Figure 4.1 show electrospun fiber mat by using NMP solvent.

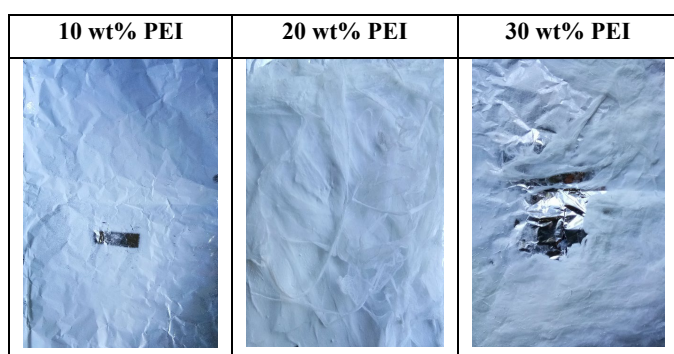


Fig. 2: Electrospun PEI fiber mat

Based on Table 1, the porosity of the electrospun PEI is increased with the increasing of the concentration of PEI solution which are 87.71 %, 88.08 %, and 90.83 % at concentration of 10 wt%, 20 wt%, and 30 wt% of PEI respectively. Thus, 30 wt% of PEI is more porous compared to the other two concentration. Moreover, porosity is also connected to the electrolyte uptake of the fiber mats. Therefore, the suitability of the concentration can be further confirmed by performing the calculation for electrolyte uptake. The calculation for the porosity and electrolyte uptake for the electrospun sample were shown in Appendix A.

Table 2 shows electrolyte uptake for the electrospun PEI. From the table, it shown that the electrolyte uptake is increased with the increasing of concentration and porosity. The higher the porosity of the fiber mats, the higher the electrolyte uptake for the fiber mats. Electrolyte uptake for 10 wt%, 20 wt%, and 30 wt% of PEI are 518.18 %, 532.78 %, and 1337.84 % respectively.

Table 1: Porosity of the Electrospun Fiber Mat

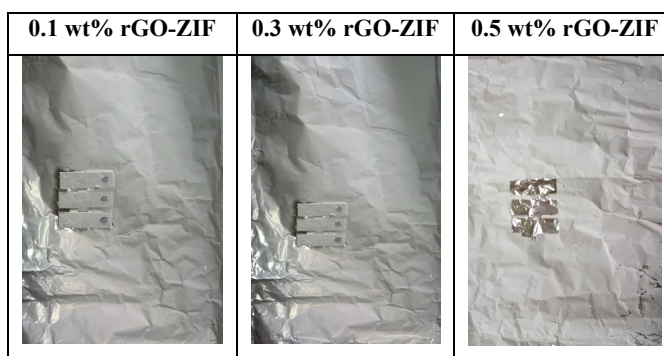
From the calculation of the porosity and electrolyte uptake, it shows that 30 wt% of PEI is the best of electrospun PEI produced. Thus, this concentration is chosen for the addition of rGO-ZIF. Fig.

Concentration of PEI (wt%)	Porosity (%)	Electrolyte Uptake (%)
10	87.77	518.18
20	88.08	532.78
30	90.83	1337.84

3 shows the electrospun fiber mats produced after the rGO-ZIF is introduced to the PEI to increase the conductivity of the PEI for the sensor application.

Fig. 3: Electrospun PEI fiber mat with addition of rGO-ZIF

The porosity of electrospun fiber after the addition of rGO-ZIF



is decreased to 84.39% for 0.1 wt% rGO-ZIF added but later the porosity increased to 92.30% for 0.3 wt% rGO-ZIF. Unfortunately, porosity is decreased again to 88.25% when the rGO-ZIF with 0.5 wt% is added. This might happen because the concentration of the rGO-ZIF used is less compared to the PEI concentration. Study conducted by [19], showed that rGO addition into the polymer will increase the porosity but the amount of rGO added should be controlled to avoid agglomeration occurred. In the research conducted by [20], it is found that rGO-ZIF combination will affect the porosity and conductivity of the material it dispersed because the ZIF will mainly affecting the porosity which it will increasing the porosity and rGO will increasing the conductivity of the material. But this combination must be added with suitable amount to achieve desired result.

Table 2 shows the result of porosity with the addition of rGO-ZIF and table 4.4 shows the result of electrolyte uptake. Porosity of 84.39%, 92.30%, and 88.25% will produce the electrolyte uptake of 781.48%, 1976%, and 1241.03% respectively. Thus, it can be conclude that electrolyte uptake will increase with the increasing of porosity.

Table 2: Porosity of the Electrospun Fiber Mat

B. Conductivity of Electrospun Fiber Mats

Concentration of 30 wt% PEI with addition of rGO-ZIF	Porosity (%)	Electrolyte Uptake (%)
0.1 wt% rGO-ZIF	84.39	781.48
0.3 wt% rGO-ZIF	92.30	1976.00
0.5 wt% rGO-ZIF	88.25	1241.03

Conductivity of the electrospun fiber is determined by using electrochemical impedance spectroscopy or known as EIS. During

electrospinning, screen-printed carbon electrode (SPCE) is attached to the foil so that the fiber mat is electrospun onto the SPCE. The frequency range used for the EIS is between 1500,000 Hz to 600 Hz for all the electrospun fiber mat. EIS will produce the result in Nyquist Plot where bulk resistance can be obtained. Thus, conductivity can be calculated using the conductivity formula where the thickness of the fiber is divide with the multiplication of bulk resistance (R_{ib}) with the area of SPCE. The bulk resistance (R_{ib}) is determined from the Nyquist Plot where the semicircle was fitted. Then, bulk resistance was calculated from the extrapolation of the semicircle on the x-axis. Besides, the y-axis and x-axis must be in equivalent scale so that the radius of the circle is same [16]. Fig. 4 shows Nyquist Plot of the resistance of electrospun fiber mat by electrospinning.

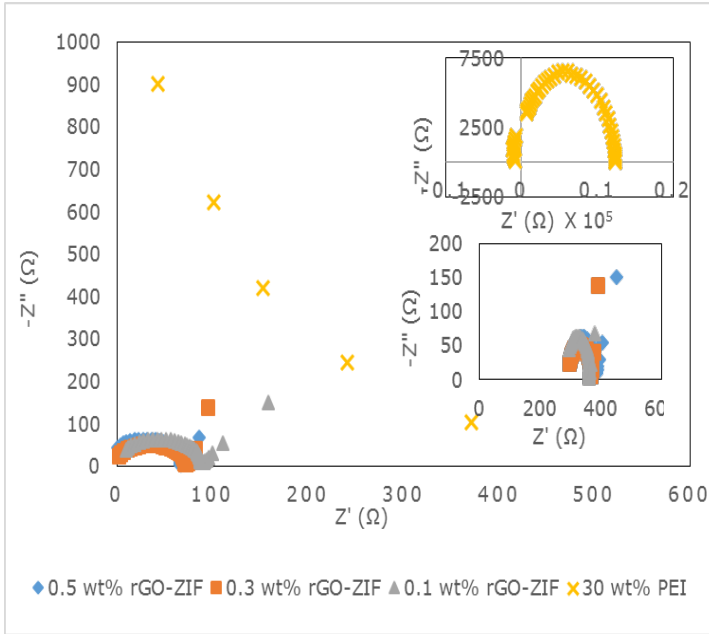


Figure 4: Nyquist Plot of the resistance of electrospun fiber mat by Electrospinning.

The Nyquist Plot from Fig 4 represented the bulk resistance of the PEI fiber mat and nanofiber by using electrospinning. Nanofiber have lower bulk resistance since the structure of the nanofiber is porous. Thus, the electrolyte uptake is also higher because porous structure can hold more electrolyte which causing the bulk resistance to lower but increasing in conductivity. From Fig 4 also, it is shown that the electrospun PEI have higher bulk resistance compared to the nanofiber which causing the conductivity of the PEI is higher than nanofiber. The nanofiber is the combination of PEI with the addition of rGO-ZIF. The figure also shows that the bulk resistance are in decreasing trend as the rGO-ZIF is added to the PEI. In the graph, the blue, orange, and gray color represented the addition of 0.1 wt% rGO-ZIF, 0.3 wt% rGO-ZIF, and 0.5 wt% rGO-ZIF respectively. Moreover, it also shows decreasing in bulk resistance from $8.92 \times 10^1 \pm 0.51 \times 10^{-3} \Omega$ to $7.61 \times 10^1 \pm 0.42 \times 10^{-1} \Omega$ as the concentration is increase from 0.1 wt% of rGO-ZIF to 0.3 wt% of rGO-ZIF and the bulk resistance is increasing again to $8.24 \times 10^1 \pm 1.97 \times 10^1 \Omega$ when the concentration of the rGO-ZIF is increasing to 0.5 wt%. From the result, it can be imply that possibly when the PEI is added with 0.3 wt% of rGO-ZIF it reach the optimum bulk resistance that cause this combination to have lower bulk resistance compared to other two concentration. Table 3 below shows the summary of the bulk resistance and conductivity of the electrospun PEI and nanofibers by electrospinning method.

Table 3: The Bulk Resistance and Conductivity of the Electrospun Fiber Mats by Electrospinning Method.

	Bulk Resistance (Ω)	Conductivity (S/cm)
30 wt% PEI	1.47×10^4 $\pm 1.62 \times 10^3$	3.08×10^{-6} $\pm 3.59 \times 10^{-7}$
0.1 wt% rGO-ZIF-30 wt% PEI	8.92×10^1 $\pm 0.51 \times 10^{-3}$	1.01×10^{-4} $\pm 5.65 \times 10^{-6}$
0.3 wt% rGO-ZIF-30 wt% PEI	7.61×10^1 $\pm 0.42 \times 10^{-1}$	2.36×10^{-4} $\pm 1.31 \times 10^{-5}$
0.5 wt% rGO-ZIF-30 wt% PEI	8.24×10^1 $\pm 1.97 \times 10^1$	1.92×10^{-4} $\pm 1.45 \times 10^{-4}$

Variation of concentration used can causing the different in conductivities of the electrospun fiber. Based on Table 3, it shows that the PEI without the addition of rGO-ZIF have lower conductivity which is $3.08 \times 10^{-6} \pm 3.59 \times 10^{-7}$ S/cm compared to the conductivity when the PEI is added with rGO-ZIF. When the PEI is added with rGO-ZIF, the conductivity is increased drastically with the increasing of concentration from 0.1 wt% of rGO-ZIF to 0.3 wt% of rGO-ZIF which are $1.01 \times 10^{-4} \pm 5.65 \times 10^{-6}$ S/cm and $2.36 \times 10^{-4} \pm 1.31 \times 10^{-5}$ S/cm respectively, and the conductivity decreasing again when the concentration further increase to 0.5 wt% of rGO-ZIF which is $1.92 \times 10^{-4} \pm 1.45 \times 10^{-4}$ S/cm. Thus, it shows that at addition of 0.3 wt% rGO-ZIF to PEI, the electrospun fiber may achieving it optimum concentration.

C. Contact Angle Analysis

One of the way to determine wettability of the surface is by using contact angle analysis. The way of the liquid dropped on a solid substrate spreads out or the capability of the liquid to produce boundary surfaces with solid states is known as wetting. This wetting is determined by contact angle in which the liquid is formed onto the solid surfaces. As the wetting trend is larger, the contact angle become smaller [21]. According to [22], the contact angle between liquid and solid is the angle inside of the liquid which is formed at the gas-liquid interface. When the contact angle is less than 90° , the liquid will wet the solid surface and spread over it while when the contact angle is more than or equal to 90° , the liquid will not spread on the solid surface and it will stay on the surface as a bead like. Moreover, the contact angle which is less than 90° is indicated as high wettability while when the angle is more than or equal to 90° it is indicating that the surface is low wettability. Besides that, when the contact angle reached 150° , the surface is known as superhydrophobic surfaces where the surfaces shows practically no contact between liquid drop and the surface and this phenomenon is known as lotus effect [23]. Thus, it is known that the low wettability and high wettability is also called hydrophobic and hydrophilic surfaces respectively. Table 4 shows the contact angle of electrospun PEI with different concentration.

Table 4: Contact Angle of Electrospun PEI

For this study, the contact angle test is conducted using the AST Products, Inc (model: VCA 3000S). From Table 4, it shows that the conditions of the electrospun PEI is hydrophobic because the contact angle is more than 90° and the electrospun PEI is also nearly to become superhydrophobic because the contact angle is

nearly to 150°. As the concentration of the PEI is increasing, the

Concentration	10 wt%	20 wt%	30 wt%
Contact angle image			
Contact angle	135.08 ± 4.65°	123.88 ± 4.46°	119.03 ± 4.16°

contact angle is decreasing. Table 4 also shows that the contact angle is decreasing from 135.08 ± 4.65°, 123.88 ± 4.46° to 119.03 ± 4.16° when the PEI concentration is increasing from 10 wt%, 20 wt% to 30 wt% respectively. According to the study from [24], structure of the electrospun mats is important in determining the hydrophobicity of the surfaces. The structure of the electrospun mats such as bead and porous is donating to the surface roughness of the mats. As the concentration of the solution is low, beads is easier to produce. Thus, the contact angle is decreases as the concentration increases. In Table 5 below shows the contact angle of electrospun PEI with the addition of rGO-ZIF in various concentration.

Table 5: Contact Angle of Electropsun PEI with the Addition of rGO-ZIF

From Table 5, it can be conclude that the contact angle of 30 wt% PEI is increasing to 121.13 ± 2.0° as the rGO-ZIF added but the contact angle is then decreasing to 111.28 ± 9.74° when the concentration of the rGO-ZIF added is increases to 0.3 wt% of rGO-ZIF. Contact angle value is increasing again to 125.45 ± 5.57° as the concentration of rGO-ZIF added increase to 0.5 wt%. The

Concentration	0.1 wt%	0.3 wt%	0.5 wt%
Contact angle image			
Contact angle	121.13 ± 2.0°	111.28 ± 9.74°	125.45 ± 5.57°

concentration of 0.1 wt % and 0.3 wt% of rGO-ZIF added to the 30 wt% PEI showed an increasing trend which make both concentration to be near superhydrophobic while the addition of 0.3 wt% rGO-ZIF to the PEI causing the contact angle to decrease and made it to be near hydrophilic characteristic.

D. FESEM Analysis

Field Emission Scanning Electron Microscopy or known as FESEM is the instrument that is used to analyze the morphology of the electrospun nanofibers. According to [25], FESEM can reach 0.6-0.7 nm electron probe diameter at 30 keV, 1.2 nm at 3 keV and 3 nm at 1.5 keV. Thus, it mean resolution which is less than 5-6 nm can be attain in lower voltage. Lower voltage of FESEM give several advantages to this instrument such as increasing the topographical contrast over more effective secondary electron (Se) gathering and reduced charging. Fig 5 and 6 below shows the FESEM image of electrospun nanofibers which is formed using electrospinning method that is captured at magnification of 5 KX and 10 KX and only 0.5 wt% rGO-ZIF added to the PEI using magnification of 3 KX and 10 KX. The FESEM image in Fig 5 are the image for electrospun PEI and in Fig 6 is the image of electrospun PEI with the addition of rGO-ZIF.

According to [12], beads can be formed by many factors such as an increase in voltage applied. When the voltage is increased, the jet velocity is also increased thus, making the solution to be remove faster from the tip. This will causing the volume of the droplet to decrease and causing the Taylor cone to be irregular and causing the bead formations. Besides, the

concentration of the solution can also effect the bead formation. Higher concentration of the solution will produced fibers with lesser beads compared to lower concentration solution. Moreover, the shape of the beads also change from spherical to spindle like as the concentration is increasing. Therefore, from Fig 5, it is shown that the electrospun nanofiber of 10 wt% PEI are producing beads compare to the 20 wt% and 30 wt% PEI. This is because 10 wt% PEI have lower concentration compare to other two. Furthermore, the fiber in 20 wt% and 30 wt% of PEI is also more uniform and smooth compare to 10 wt%.

Fig 6 on the other hand showing the FESEM image of the electrospun nanofiber of 30 wt% PEI with the addition of rGO-ZIF. Comparing the fiber at 30 wt% PEI and when adding rGO-ZIF, it is shown a huge difference where the fiber become thinner as the concentration of rGO-ZIF is increased. Unfortunately, the beads is also formed as the concentration of rGO-ZIF is increased. Concentration of the rGO-ZIF must be added appropriately because at some point, increasing of rGO-ZIF concentration will make the beads become more visible and spindle like because the charge density is increased.

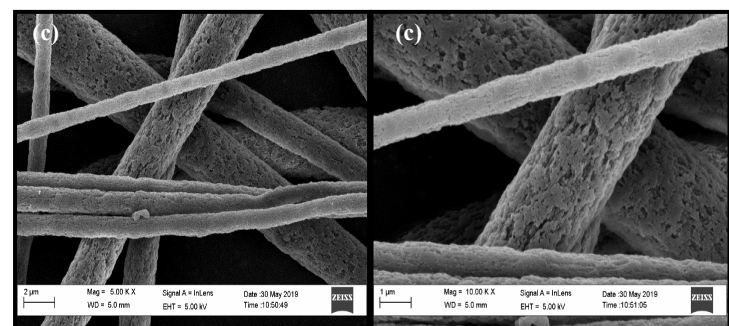
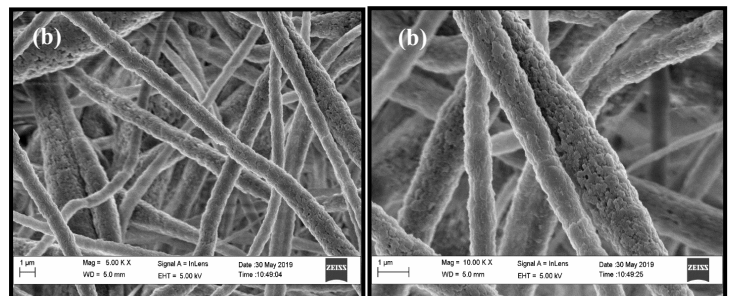
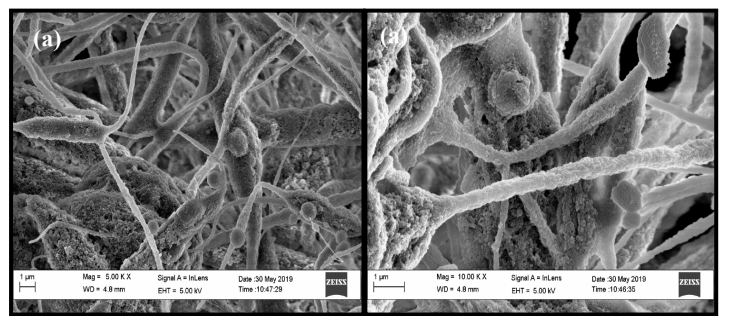
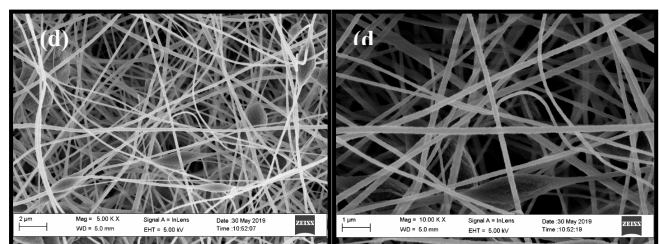


Fig 5: FESEM images of electrospun PEI at magnification of 5 KX and 10 KX (a) electrospun PEI of 10 wt% (b) Electrospun PEI of 20 wt% (c) Electrospun PEI of 30 wt%



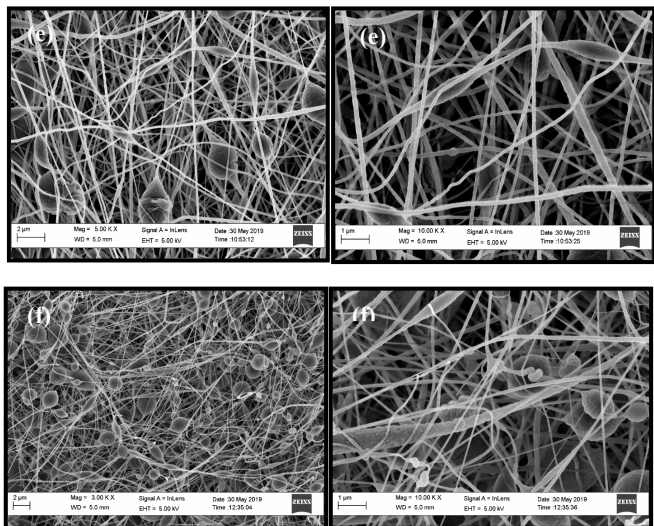


Fig 6: FESEM images of electrospun PEI with the addition of rGO-ZIF (d) 30 wt% PEI + 0.1 wt% rGO-ZIF at magnification 5 KX and 10 KX (e) 30 wt% PEI + 0.3 wt% rGO-ZIF at magnification 5 KX and 10 KX (f) 30 wt% PEI + 0.5 wt% rGO-ZIF at magnification 3 KX and 10 KX

Figs 6 and 7 show the particle size distribution histogram of the electrospun PEI and the electrospun PEI with the addition of rGO-ZIF. From Fig 6, it shows the increasing trend of mean fiber diameter when the concentration of the PEI is increased which is 569.691 nm, 787.497 nm and 874.721 nm for 10 wt%, 20 wt% and 30 wt% of PEI respectively. Even though, the mean diameter at 10 wt% of PEI is smaller but there is bead formation for the fibers compared to other two concentration which there is no beads forming and this is causing the 10 wt% PEI is not favorable. This is because the formation of beads can causing the fiber to become rough and thus increase it diameter at certain amount. Moreover, incomplete drying of the solution when reaching to the collector because of the jet is also can causing fibers with bead [11]. At 30 wt% PEI, the fiber showing no beads but the diameter is increasing. This probably because of the higher the concentration of the polymer used, the bigger the diameter of the fiber become because the fibers may consists of bundles of single fibers. As stated by the research of [26], the formation of the bundles of single fibers may be causing by the amount of nanofibers in the space between the spinning and the collector which causing the entanglement and attaching of the single fibers. In the research of [27], it been found that the lower the feeding rate used in electrospinning, the smaller the fibers formed. The lowest feeding rate used in that research is 1.2 mL/h and the highest is 4.5 mL/h. Thus, in this research, the amount of feeding rate used is much lower compared to Zong research. Which is 0.8 mL/h. This may causing the smaller fibers with spindle-like beads formed in nanofibers which is added with rGO-ZIF.

However, for the addition of the rGO-ZIF, the PEI concentration chosen is 30 wt%. Even though the fiber diameter is higher compare to other two concentration, the conductivity is higher in the 30 wt% PEI which is the aim for this research. From Fig 7, it is shown that by adding the rGO-ZIF into the 30 wt% PEI solution, the fiber diameter decreased drastically from 874.721 nm to 216.757 nm, 179.789 nm, and 102.119 nm for the addition of 0.1 wt%, 0.3 wt% and 0.5 wt% of rGO-ZIF respectively. The fiber diameter is showing an decreasing trend as the concentration of the rGO-ZIF is increased. At 0.5 wt% of rGO-ZIF added, the fiber is thinner compared with other two concentration of rGO-ZIF. In spite of this, the bead forming is increasing for this concentration. Though the fiber diameter is thinner, 0.5 wt% of rGO-ZIF is not the best fiber diameter because the conductivity that it produce is lower than 0.3 wt% of rGO-ZIF. Thus, 0.3 wt% of rGO-ZIF is chosen as probably the most suitable addition of the PEI and the fiber diameter is also in between of the 0.1 wt and 0.5 wt% of rGO-

ZIF which is 178.789 nm. The fiber is also thinner with less bead forming.

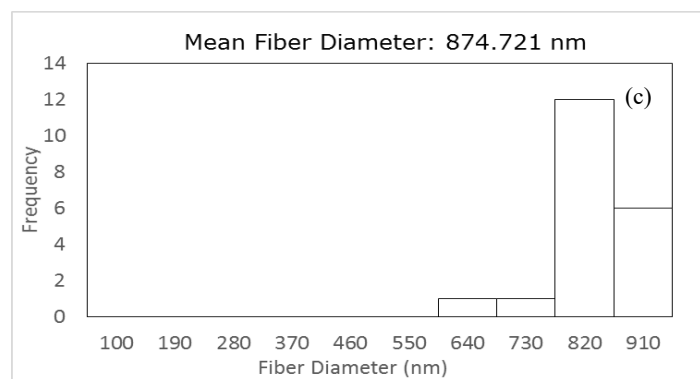
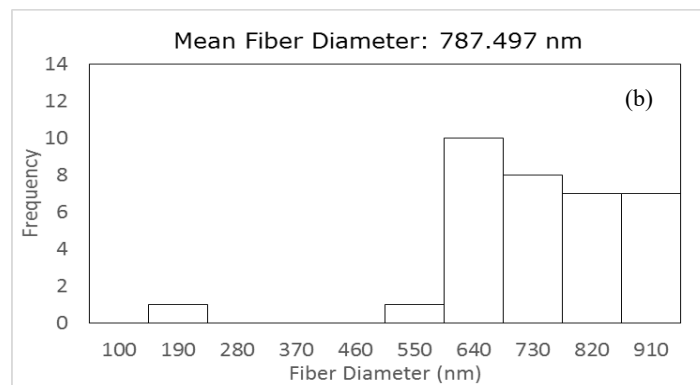
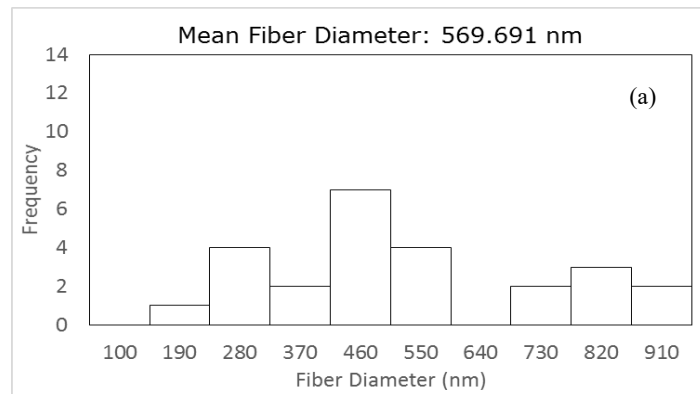
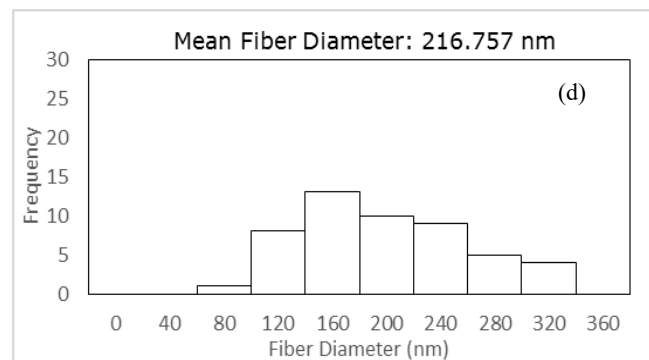


Fig 6: Particle Size Distribution Histogram for Electrospun PEI (a) at 10 wt% PEI (b) at 20 wt% PEI (c) at 30 wt% PEI



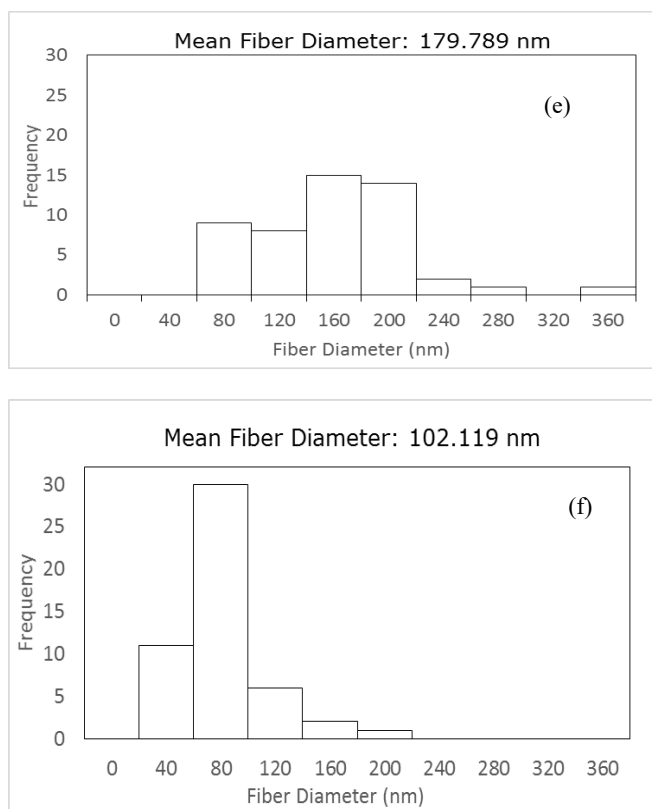


Fig 7: Particle Size Distribution Histogram for Electrospun PEI with the addition of rGO-ZIF (d) 30 wt% PEI + 0.1 wt% rGO-ZIF (e) 30 wt% PEI + 0.3 wt% rGO-ZIF (f) 30 wt% PEI + 0.5 wt% rGO-ZIF

IV. CONCLUSION

As a conclusion, it is found that PEI solution which is combined with NMP solvents will produce electrospun fiber mats with high porosity which is 90.83 % for the 30 wt % of PEI concentration and with the addition of rGO-ZIF, the electrospun fiber can achieve high porosity when 0.3 wt % of rGO-ZIF is used which the porosity is 92.30 %. Thus, it possible to say that addition of rGO-ZIF will increasing the porosity by using the suitable amount of rGO-ZIF added. Moreover, the conductivity analysis also showed an increase of conductivity from $1.01 \times 10^{-4} \pm 5.65 \times 10^{-6}$ S/cm to $2.36 \times 10^{-4} \pm 1.31 \times 10^{-5}$ S/cm for concentration of 0.1 wt % and 0.3 wt % of rGO-ZIF added, but then the concentration is decreased to $1.92 \times 10^{-4} \pm 1.45 \times 10^{-4}$ S/cm when the concentration increased to 0.5 wt %. This is because the rGO-ZIF has achieved optimum conductivity at 0.3 wt % of rGO-ZIF and this also support the porosity result of this concentration. To further clarified whether addition of 0.3 wt% rGO-ZIF is most suitable electrospun fiber for sensor, contact angle analysis is conducted. From contact angle analysis, it is discovered that the electrospun PEI mats is having hydrophobic behavior and the contact angle value is decreasing as the concentration of the PEI is increasing which are from $135.08 \pm 4.65^\circ$, $123.88 \pm 4.46^\circ$ to $119.03 \pm 4.16^\circ$ for 10 wt%, 20 wt%, and 30 wt% of PEI respectively. As the rGO-ZIF is added, the contact angle is also decreasing with the increasing of the concentration from 0.1 wt% to 0.3 wt% of rGO-ZIF. Thus, it is shown that electrospun fiber is optimum at 0.3 wt% of rGO-ZIF added because as the concentration further increases, the contact angle is increasing to be near superhydrophobic. Besides, from the FESEM result it is shown that the fiber diameter of 30 wt% PEI showing a drastic decreasing when rGO-ZIF is added to the solution. The fiber become thinner when adding with rGO-ZIF although some spindle like beads are forming. From all of the analysis result, it possible to conclude that electrospun PEI of 30 wt% with the addition of 0.3 wt% rGO-ZIF is suitable for metal sensing though the porosity and conductivity is increased, it may not be enough to

be used for sensor. Further optimization of the fibers must be done to produce the selective sensor that can detect heavy metal.

ACKNOWLEDGMENT

Thank you to my supervisor and Universiti Teknologi Mara.

REFERENCES

- [1] D. Vilela, J. Parmar, Y. Zeng, Y. Zhao, and S. Sánchez, "Graphene-Based Microbots for Toxic Heavy Metal Removal and Recovery from Water," *Nano Lett.*, vol. 16, no. 4, pp. 2860–2866, 2016.
- [2] Y. Liu, Y. Deng, H. Dong, K. Liu, and N. He, "Progress on sensors based on nanomaterials for rapid detection of heavy metal ions," *Sci. China Chem.*, vol. 60, no. 3, pp. 329–337, 2017.
- [3] V. Ishchenko and I. Vasylykivskyi, *Environmental Pollution with Heavy Metals: Case Study of the Household Waste*. Springer International Publishing, 2020.
- [4] A. Mičijević, A. Šukalić, and A. Leto, *New Technologies, Development and Application II*, vol. 76, no. 76. Cham: Springer International Publishing, 2020.
- [5] X. Fang, B. Zong, and S. Mao, "Metal–Organic Framework-Based Sensors for Environmental Contaminant Sensing," *Nano-Micro Lett.*, vol. 10, no. 4, pp. 2–19, 2018.
- [6] M. Li, H. Gou, I. Al-Ogaidi, and N. Wu, "Nanostructured Sensors for Detection of Heavy Metals: A Review," *ACS Sustain. Chem. Eng.*, vol. 1, no. 7, pp. 713–723, Jul. 2013.
- [7] Q. A. Drmosh *et al.*, "A novel approach to fabricating a ternary rGO/ZnO/Pt system for high-performance hydrogen sensor at low operating temperatures," *Appl. Surf. Sci.*, vol. 464, pp. 616–626, 2018.
- [8] B. Chen, Z. Yang, Y. Zhu, and Y. Xia, "Zeolitic imidazolate framework materials: Recent progress in synthesis and applications," *Journal of Materials Chemistry A*, vol. 2, no. 40. Royal Society of Chemistry, pp. 16811–16831, 2014.
- [9] Y. Pan, Y. Liu, G. Zeng, L. Zhao, and Z. Lai, "Rapid synthesis of zeolitic imidazolate framework-8 (ZIF-8) nanocrystals in an aqueous system," *Chem. Commun.*, vol. 47, no. 7, pp. 2071–2073, 2011.
- [10] C. Wang *et al.*, "In Situ Growth of ZIF-8 on PAN Fibrous Filters for Highly Efficient U(VI) Removal," *ACS Appl. Mater. Interfaces*, vol. 10, no. 28, pp. 24164–24171, 2018.
- [11] S. Saallah, M. N. Naim, M. N. Mokhtar, N. F. A. Bakar, M. Gen, and I. W. Lenggono, "Preparation and Characterisation of Cyclodextrin Glucanotransferase Enzyme Immobilised in Electrospun Nanofibrous Membrane," *J. Fiber Sci. Technol.*, vol. 73, no. 10, pp. 251–260, 2017.
- [12] K. Garg and G. L. Bowlin, "Electrospinning jets and nanofibrous structures," *Biomicrofluidics*, vol. 5, no. 1, 2011.
- [13] D. M. Sato, L. M. Guerrini, M. P. de Oliveira, L. R. de O. Hein, and E. C. Botelho, "Production and characterization of polyetherimide mats by an electrospinning process," *Mater. Res. Express*, vol. 5, no. 11, p. 115302, Sep. 2018.
- [14] J. Ling, W. Zhai, W. Feng, B. Shen, J. Zhang, and W. G. Zheng, "Facile preparation of lightweight microcellular polyetherimide/graphene composite foams for electromagnetic interference shielding," *ACS Appl. Mater. Interfaces*, vol. 5, no. 7, pp. 2677–2684, 2013.
- [15] N. Jamil *et al.*, "Mixed matrix membranes incorporated with reduced graphene oxide (rGO) and zeolitic imidazole framework-8 (ZIF-8) nanofillers for gas separation," *J. Solid State Chem.*, vol. 270, pp. 419–427, 2019.
- [16] K. W. Chew, T. C. Ng, and Z. H. How, "Conductivity and microstructure study of PLA-based polymer electrolyte salted with lithium perchlorate, LiClO₄," *Int. J. Electrochem. Sci.*, vol. 8, no. 5, pp. 6354–6364, 2013.
- [17] T. Wang, W. Dong, and Y. Chen, "Study on Porosity of Electrospun Nanofiber Membrane by Neural Network," vol. 12, no. 22, pp. 1059–1074, 2018.
- [18] N. Bhardwaj and S. C. Kundu, "Electrospinning: A fascinating fiber fabrication technique," *Biotechnol. Adv.*, vol. 28, no. 3, pp. 325–347, 2010.
- [19] V. Vatanpour, A. Shockravi, H. Zarrabi, Z. Nikjavan, and A. Javadi, "Fabrication and characterization of anti-fouling and anti-bacterial Ag-loaded graphene oxide/polyethersulfone mixed

- matrix membrane,” *J. Ind. Eng. Chem.*, vol. 30, pp. 342–352, 2015.
- [20] G. Yu, J. Xia, F. Zhang, and Z. Wang, “Hierarchical and hybrid RGO/ZIF-8 nanocomposite as electrochemical sensor for ultrasensitive determination of dopamine,” *J. Electroanal. Chem.*, vol. 801, no. August, pp. 496–502, 2017.
- [21] C. Dwivedi, I. Pandey, H. Pandey, and P. W. Ramteke, *Electrospun Nanofibrous Scaffold as a Potential Carrier of Antimicrobial Therapeutics for Diabetic Wound Healing and Tissue Regeneration*. Elsevier Inc., 2017.
- [22] S. Micelles, A. Surfactants, C. Surfactants, N. Surfactants, S. P. Enhancers, and E. Agents, “Surfactants , Lipids , and Surface Chemistry,” *Essent. Chem. Formul. Semisolid Liq. Dos.*, pp. 5–19, 2016.
- [23] Y. Yuan and T. R. Lee, “Contact Angle and Wetting Properties,” in *Surface Science Techniques*, vol. 51, 2013, pp. 3–33.
- [24] S. Huan *et al.*, “Effect of Experimental Parameters on Morphological, Mechanical and Hydrophobic Properties of Electrospun Polystyrene Fibers,” *Materials (Basel)*, vol. 8, pp. 2718–2734, 2015.
- [25] S. L. Erlandsen, C. Frethem, and Y. Chen, “Field Emission Scanning Electron Microscopy (FESEM) Entering the 21st Century: Nanometer Resolution and Molecular Topography of Cell Structure,” *J. Histotechnol.*, vol. 23, no. 3, pp. 249–259, 2014.
- [26] F. Yener and O. Jirsak, “Comparison between the Needle and Roller Electrospinning of Polyvinylbutyral,” *J. Nanomater.*, vol. 2012, pp. 1–6, 2012.
- [27] X. Zong, K. Kim, D. Fang, S. Ran, B. S. Hsiao, and B. Chu, “Structure and process relationship of electrospun bioabsorbable nanofiber membranes,” *Polymer (Guildf)*, vol. 43, no. 16, pp. 4403–4412, Jul. 2002.